

Supplementary Information for

Intricate carrier dynamics of bismuth halide perovskites: localized excitons and polarons

Naveen Kumar Tailor,^{1,2} Sanchi Monga,³ Saurabh K. Saini^{4,5}, Mahesh Kumar^{5,6}, Saswata
Bhattacharya,^{3,*} Soumitra Satapathi^{1,2,*}

¹*Department of Physics, Indian Institute of Technology Roorkee, Roorkee 247667, India*

²*Center for Sustainable Energy, Indian Institute of Technology Roorkee, Roorkee 247667, India*

³*Department of Physics, Indian Institute of Technology Delhi, Hauz Khas, New Delhi 110016, India*

⁴*CSIR-National Physical Laboratory, Dr. K.S. Krishnan Marg, New Delhi, 110012 India*

⁵*Academy of Scientific and Innovative Research (AcSIR), Ghaziabad, 201002 India*

⁶*Innovation Management Directorate, Anusandhan Bhawan, New Delhi 110001*

*Corresponding Author: saswata@physics.iitd.ac.in, soumitrasatapathi@gmail.com

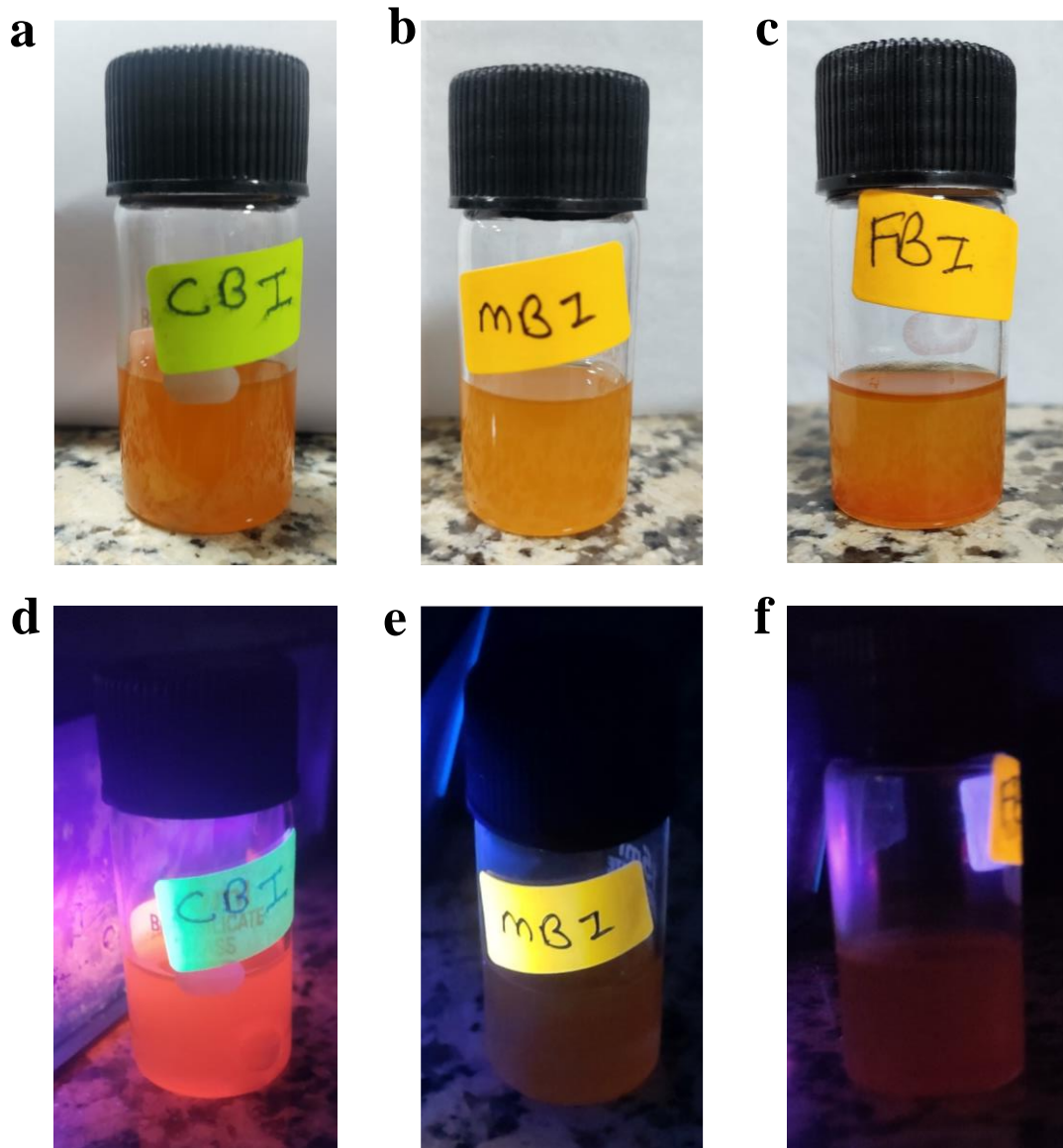


Figure S1. (a) Image of fabricated nanocrystals $\text{Cs}_3\text{Bi}_2\text{I}_9$, $\text{MA}_3\text{Bi}_2\text{I}_9$, and $\text{FA}_3\text{Bi}_2\text{I}_9$. (b) Image under UV light illumination.

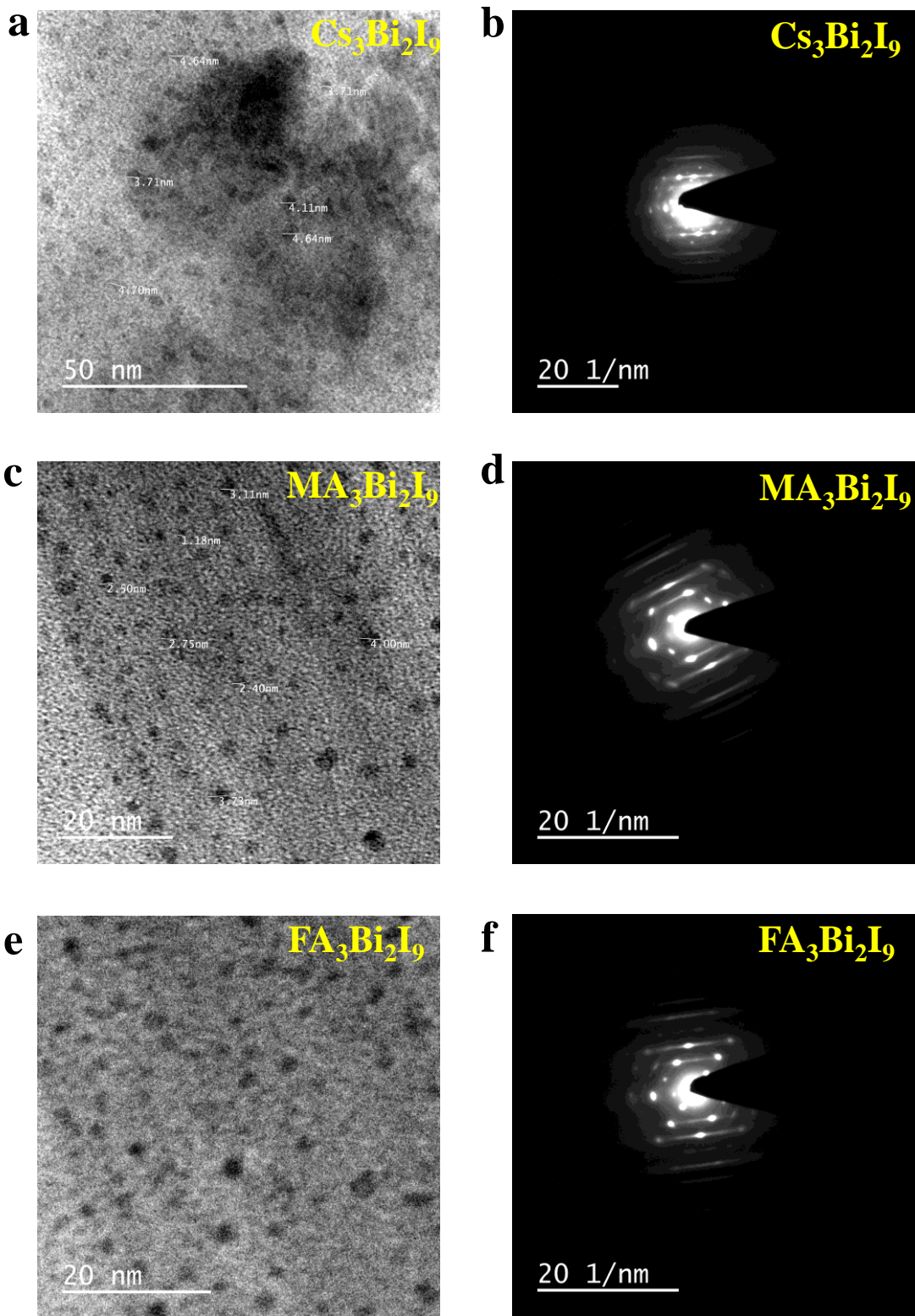


Figure S2. TEM image of the (a) $\text{Cs}_3\text{Bi}_2\text{I}_9$ NCs, (c) $\text{MA}_3\text{Bi}_2\text{I}_9$ NCs, (e) $\text{MA}_3\text{Bi}_2\text{I}_9$ NCs. Reciprocal pattern of (b) $\text{Cs}_3\text{Bi}_2\text{I}_9$ NCs, (d) $\text{MA}_3\text{Bi}_2\text{I}_9$ NCs, and (f) $\text{FA}_3\text{Bi}_2\text{I}_9$ NCs.

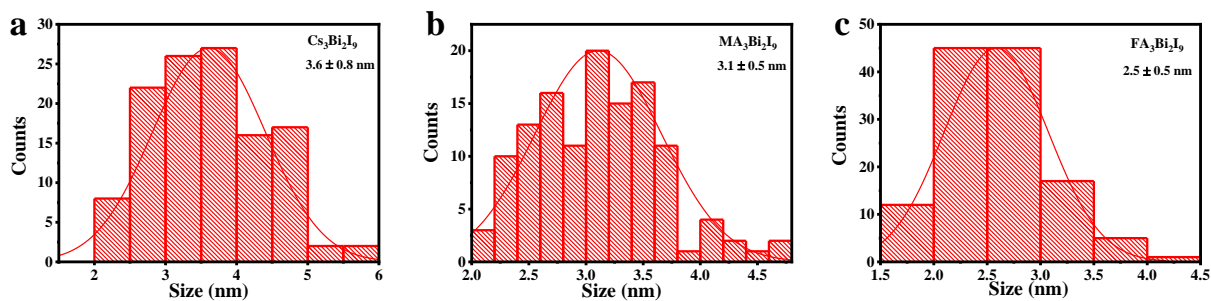


Figure S3. Size distribution of (a) $\text{Cs}_3\text{Bi}_2\text{I}_9$ NCs, (b) $\text{MA}_3\text{Bi}_2\text{I}_9$ NCs and (c) $\text{FA}_3\text{Bi}_2\text{I}_9$ NCs.

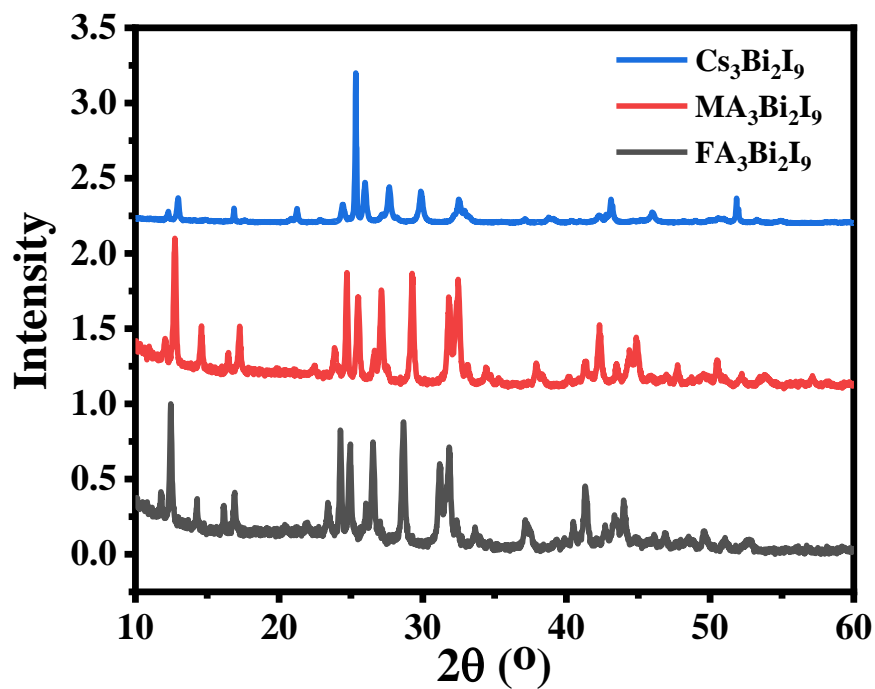


Figure S4. Powder XRD pattern of fabricated nanocrystal $\text{Cs}_3\text{Bi}_2\text{I}_9$, $\text{MA}_3\text{Bi}_2\text{I}_9$, and $\text{FA}_3\text{Bi}_2\text{I}_9$ powder.

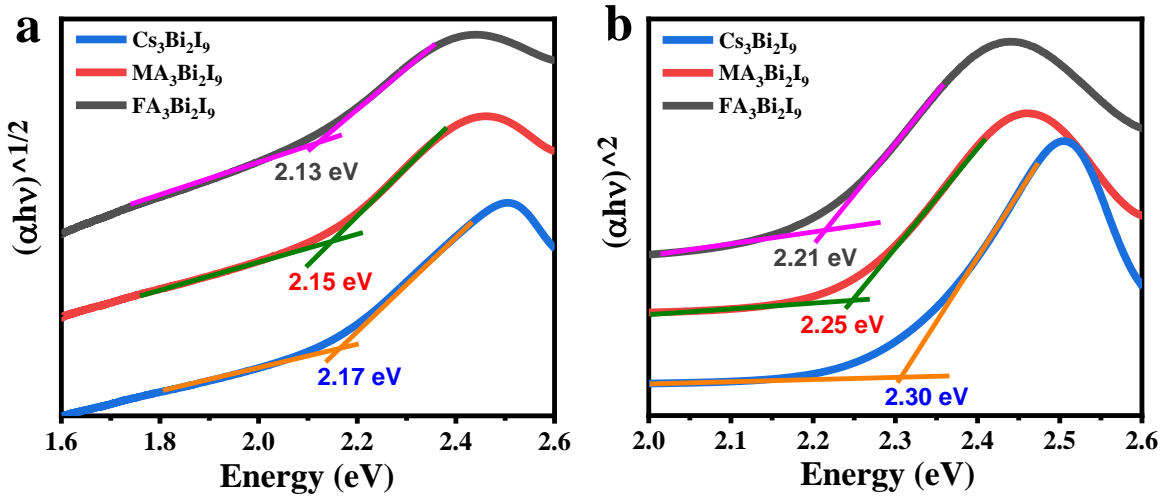


Figure S5. Calculated bandgap from tauc plot method. (a) indirect bandgap and (b) direct bandgap for all three systems.

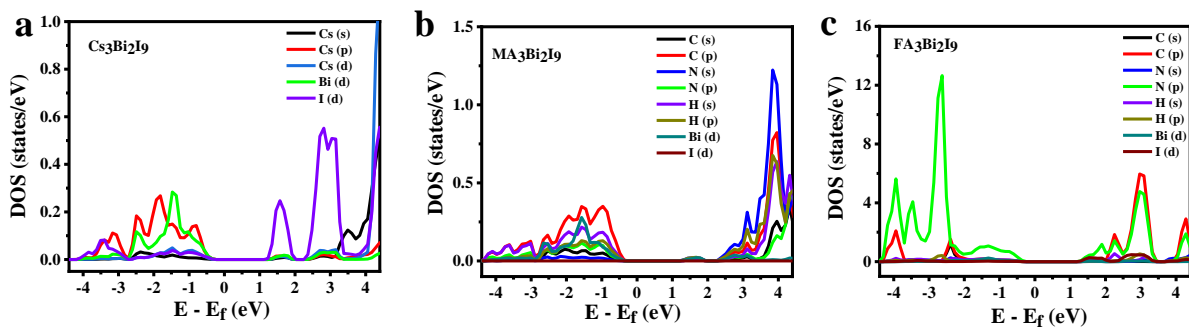


Figure S6. Atom-projected partial density of states (pDOS) for (a) $\text{Cs}_3\text{Bi}_2\text{I}_9$ (b) $\text{MA}_3\text{Bi}_2\text{I}_9$ and (c) $\text{FA}_3\text{Bi}_2\text{I}_9$.

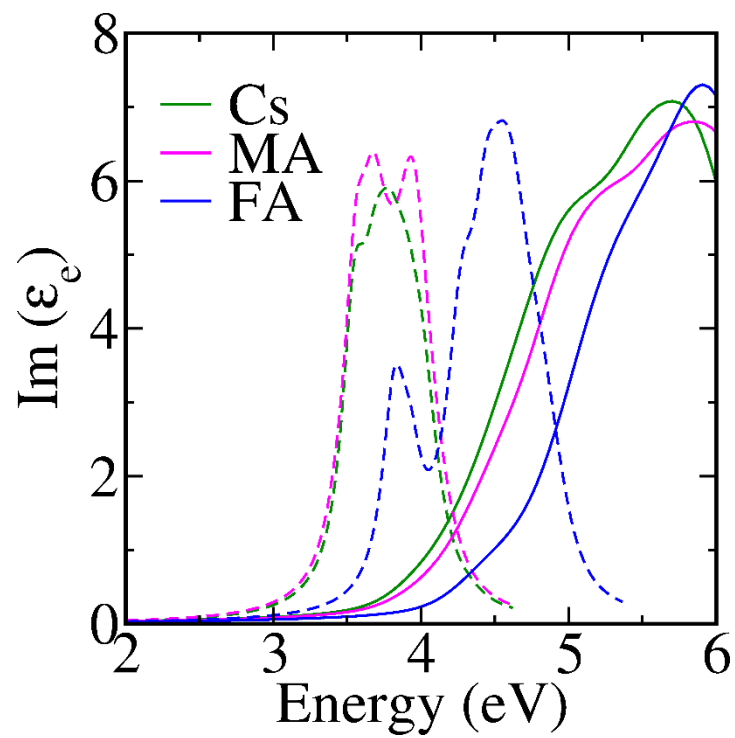


Figure S7. Electronic (solid) and optical spectra (dotted) of $\text{Cs}_3\text{Bi}_2\text{I}_9$, $\text{MA}_3\text{Bi}_2\text{I}_9$, and $\text{FA}_3\text{Bi}_2\text{I}_9$, estimated using G_0W_0 and mBSE on top of PBE exchange-correlation functional.

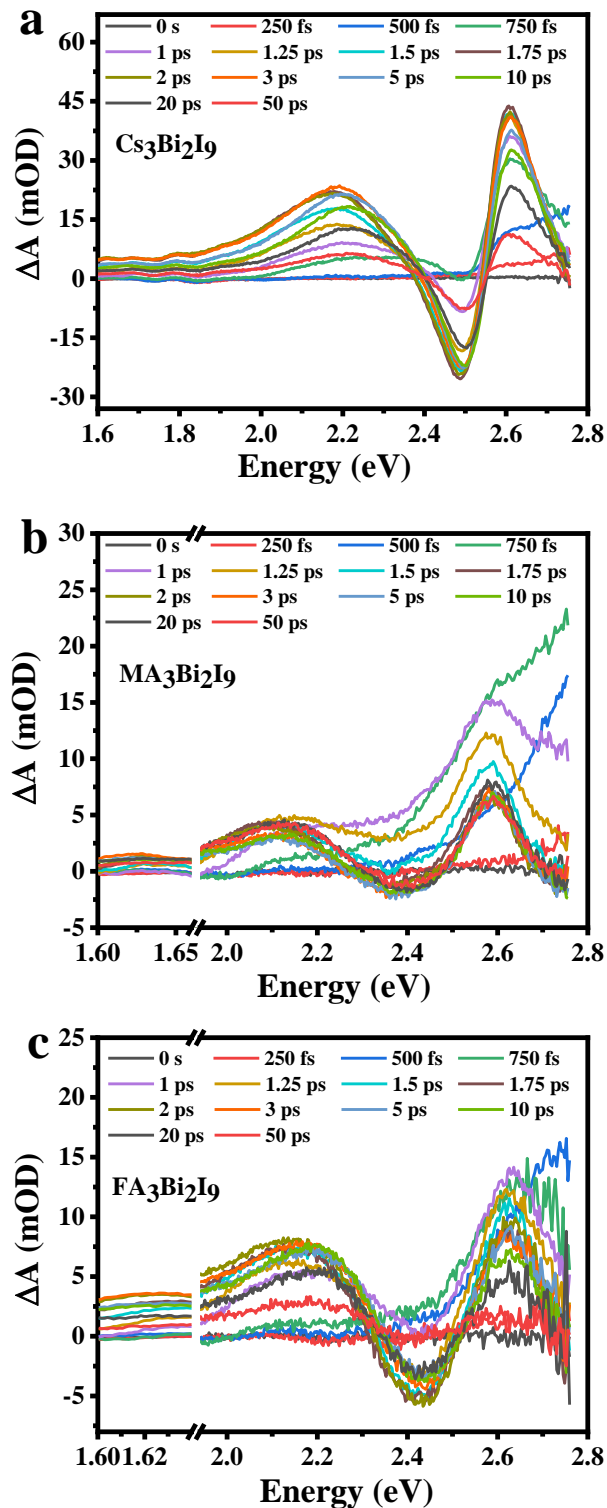


Figure S8. Femtosecond transient absorption (fs-TA) spectra in response to 350 nm optical excitation. Early time spectra up to 50 ps for (a) $\text{Cs}_3\text{Bi}_2\text{I}_9$, (b) $\text{MA}_3\text{Bi}_2\text{I}_9$, and (c) $\text{FA}_3\text{Bi}_2\text{I}_9$.

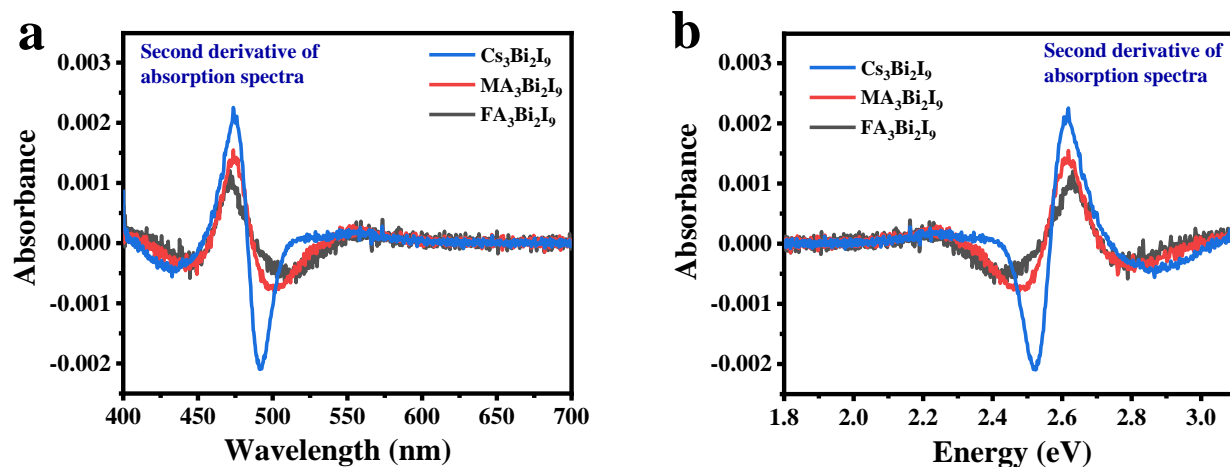


Figure S9. Smoothed second derivative of the steady-state absorption spectrum of $\text{Cs}_3\text{Bi}_2\text{I}_9$, $\text{MA}_3\text{Bi}_2\text{I}_9$, and $\text{FA}_3\text{Bi}_2\text{I}_9$ (a) wavelength scale and (b) energy scale.

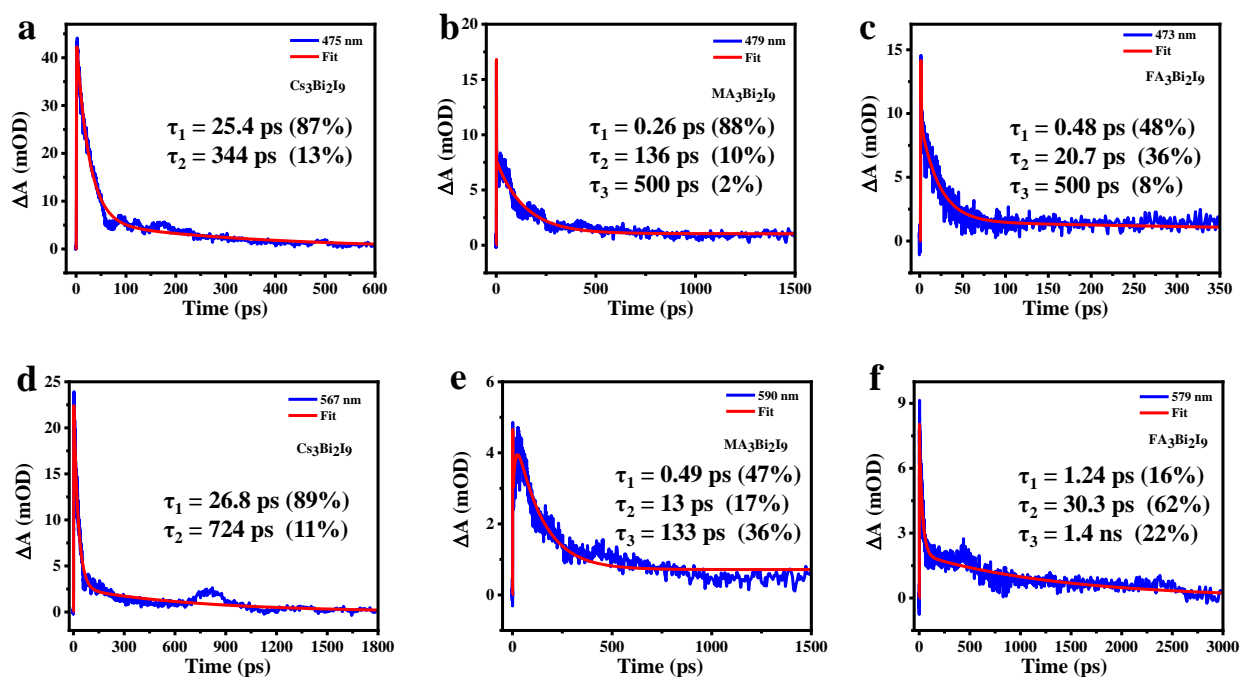


Figure S10. Kinetics at different probe wavelengths for all three systems. (a) $\text{Cs}_3\text{Bi}_2\text{I}_9$ at 475 nm, (b) $\text{MA}_3\text{Bi}_2\text{I}_9$ at 479 nm, (c) $\text{FA}_3\text{Bi}_2\text{I}_9$ at 473 nm, (d) $\text{Cs}_3\text{Bi}_2\text{I}_9$ at 567 nm, (e) $\text{MA}_3\text{Bi}_2\text{I}_9$ at 590 nm, (f) $\text{FA}_3\text{Bi}_2\text{I}_9$ at 579 nm.